

COVER PAGE

Document downloaded by @DAEL

Sat Nov 28 08:56:11 2026
For personal use

When automatic English translation is provided, only the original document is authentic.
The EAA cannot be held responsible of any translation error

Bibliographical reference

Impulsive Noise Detection in Sweep Measurements, M. Guski and M. Vorländer, Acta Acustica **vol. 101** (Number 4), 2015, pp. 723-730

DOI
https://doi.org/10.3813/AAA.918868

Acta Acustica united with Acustica
Vol. 101 (2015) 723 – 730

DOI 10.3813/AAA.918868

Impulsive Noise Detection in Sweep Measurements

M. Guski, M. Vorländer
Institute of Technical Acoustics, RWTH Aachen University, Kopernikusstraße 5, 52074 Aachen, Germany.
mgu@akustik.rwth-aachen.de

Summary
Sweeps used as excitation signals for impulse response measurements show various advantages compared to other excitation signals regarding time variances, non-linearities and signal to noise ratio. The main disadvantage of sweeps is the sensitivity to impulsive noise during the measurement, because the noise affects specific frequencies with rather high noise levels. The fact that the occurrence of impulsive noise is hard to detect complicates the problem. Maximum length sequence or similar techniques, where the signal excites all frequencies (pseudo-)randomly, are more robust against impulsive noise, because any kind of background noise is spread over the full time range of the impulse response with relatively low levels. In this paper a detection method for impulsive noise in sweep measurements is presented. The excitation signal is removed from the recorded signal to obtain an estimation of the background noise during the measurement. In this processed signal the impulsive noise is clearly visible against the stationary background noise. After the measurement, this detection can be automatically executed and allows a repetition of measurement, if necessary.

PACS no. 43.55.Mc, 43.55.Br

1. Introduction

The common way to measure room impulse responses (RIR) is to excite the sound field with a loudspeaker and record the signal at the receiver position using a microphone. The choice of the excitation signal for the loudspeaker has a significant influence on the quality of the result. Sine sweeps (also known as chirps or time-stretched pulses) offer several advantages compared to other excitation signals such as maximum length sequences (MLS) or random noise [1, 2]. Since for sweeps every frequency is excited during a relatively short moment, time variances in the system (for example air movement in the room or temperature changes of an amplifier/transducer device or the room) result only in small errors. For MLS and noise measurements all frequencies are excited randomly in the entire measurement time, and the resulting transfer function is an average of these conditions and might include inaccuracies by superposition effects of those variances.

Sweeps are advantageous, too, when applied to slightly nonlinear systems [1, 2]. For exponential sweeps (sometimes also called logarithmic sweeps), the main parts of the individual harmonic components appear at well determined positions in the measured impulse response. This allows a direct estimation of the nonlinearities' magnitude and a removal of these major nonlinear components using time windows. For MLS and noise measurements, the nonlinear components appear as peaks spread over the complete measured block.

Sweeps provide a robust signal to noise ratio for stationary noise conditions, similar to those in MLS or random noise measurements with FFT-based deconvolution [2].

Impulsive noise during a measurement is often caused by sources such as creaking wooden floors or beams, footsteps of people in the room, or coughing. In MLS or random noise measurements, impulsive noise is transformed into a relatively low-level random noise component in the measured response, and thus it has only small influences on further processing steps. Nevertheless, this noise is spread over all frequencies and the the full period of the RIR. In contrast, for sweep signals the transient (impulsive) disruption results in a deterministic artifact in the measured impulse responses that distorts evaluation and auralization[1, 3]. Up to now, there exist no reliable method for identification and evaluation of impulsive noise in sweep measurements.

In this study, the automatic detection of impulsive noise in sweep measurements is described. Farina [4] showed that it is possible to properly reduce the effects of impulsive noise only by individual treatment of every measurement while automatic methods give insufficient results. A robust automatic compensation of the disruption, however, could not be found yet and will be subject to further research. The presented detection technique can be used for any excitation signal, but, due to the high sensitivity of sweeps to impulsive noise, it is especially important for

Received 11 July 2014,
accepted 26 January 2015.

© S. Hirzel Verlag · EAA

sweep measurements. The technique can be used to automatically analyze the measured response immediately after the affected measurement and to repeat the measurement period, if necessary.

All simulations, measurements, room acoustic evaluation, and data processing are done using the ITA-Toolbox [5]. The ITA-Toolbox is an open source toolbox for Matlab. It includes a script (ita_tutorial_impulsive_noise.m) to reproduce all results of the following chapter.

2. Theory

For illustration purpose in this chapter, a simulated impulse response is used. A rectangular room with a reverberation time of 1.5 seconds is simulated with a modal superposition approach for a specified source and receiver position. Figure 1 (top) shows the RIR using a logarithmic scale (also known as energy room-impulse response or echogram).

There are two noise components in the model: The stationary noise is unavoidable and therefore always included in the simulation, while the impulsive noise only occurs occasionally and has to be detected (see Figure 1 bottom).

The impulsive noise is modeled as a Dirac pulse and the influence of the room is considered by simulating its impulse response from a different position, far away from the actual source position. Ambient and electro-acoustic equipment noise is modeled as Gaussian white noise. This approach allows controlling the conditions and observing the effects in every processing step for every signal component (excitation signal and impulsive noise) separately. The excitation signal is an exponential sweep with a constant envelope,

$$s(t) = \sin\left(2\pi f_1 \left(\exp\left(\frac{t}{L}\right) - 1\right)\right). \tag{1}$$

The sweep covers a frequency range from f_1 to f_2 with the parameter of exponential increase in frequency $L = T/\log(\frac{f_2}{f_1})$ and T, the length of the sweep signal. The recorded signal $r_m(t)$ at a microphone position in a room is a combination of the occurring noise $n(t)$ and the excitation signal modified by room $h(t)$,

$$r_m(t) = s(t) * h(t) + n(t). \tag{2}$$

To obtain the desired impulse response of the system, the recorded signal has to be convolved with the deconvolution signal $c(t)$ (also known as compensation signal). The deconvolution signal is the one with the inverted complex spectrum of the excitation signal. For the commonly used exponential sweep with constant envelope (Eq. (1)), the deconvolution signal is a time-reversed exponential sweep with an exponentially decreasing envelope [6], called inverse sweep (see Figure 2).

The measured impulse response $h_m(t)$ can be derived from

$$h_m(t) = \underbrace{s(t) * c(t)}_{\delta(t)} * h(t) + n(t) * c(t). \tag{3}$$

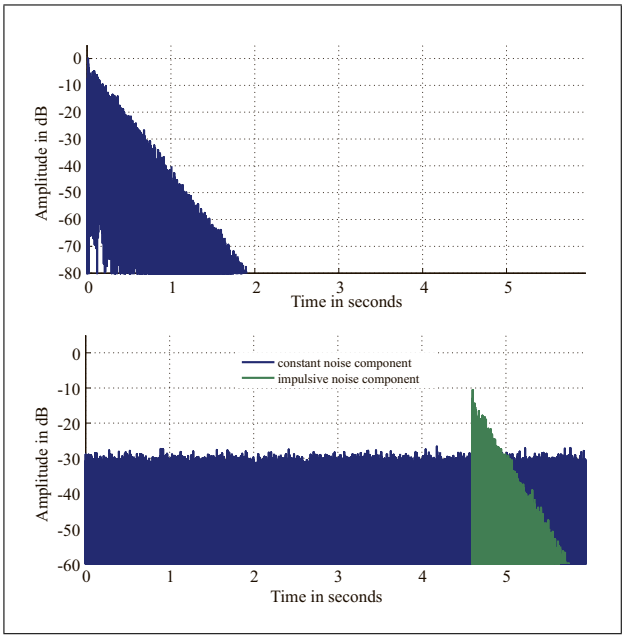


Figure 1. Top: Simulated energy RIR without any noise component. Bottom: Two noise components. The stationary noise is unavoidable (blue) and the impulsive noise component (green) has to be discovered. Colours in the online version only.

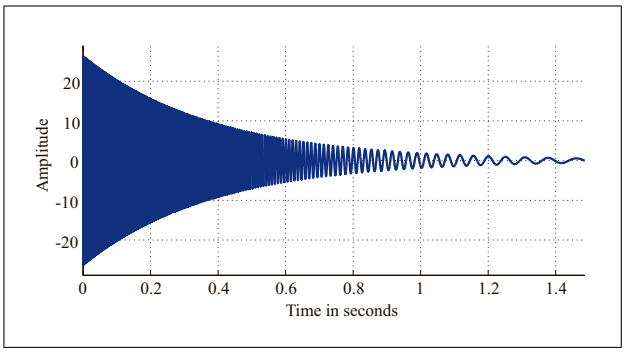


Figure 2. The inverse sweep is the deconvolution signal for the exponential sweep with constant envelope. The envelope is not constant but exponentially decreasing.

The convolution of excitation signal $s(t)$ and deconvolution signal $c(t)$ ideally results in a Dirac pulse, and thus the impulse response $h(t)$ of the system is obtained. The additive noise term is composed by the recorded background noise convolved with the inverse sweep.

The upper left part of Figure 3 shows a spectrogram (frequency on the vertical axis and time on the horizontal axis) of the impulse response without impulsive noise. The impulse on the left (red part) decays into the Gaussian background noise (blue part).

The upper right side of Figure 3 shows the contribution of the impulsive noise which is expressed by the second summand in Equation (3). Impulsive components in the recorded noise signal $n(t)$ will result in delayed representations of the deconvolution signal (the inverse sweep) in the measured impulse response.

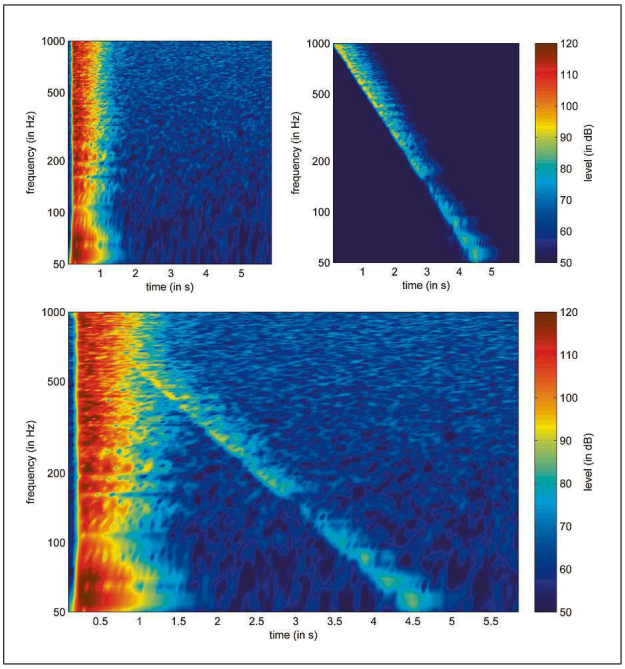


Figure 3. Top: Spectrogram of the impulse response without impulsive component on the left and inverse sweep caused by impulsive noise on the right side. Bottom: Impulse response including the inverse sweep caused by the impulsive noise.

A measurement disturbed by impulsive noise is now simulated by superpositioning both components shown in the upper part of Figure 3 is depicted in the lower part.

The deterministic structure of the interference in the impulse response is more problematic than the typical statistic random noise contained in the (stationary and broadband) blue part of the spectrogram. Figure 5 shows the reverberation time T_{20} evaluated for the undisturbed (blue) and the disturbed impulse response (green). For the room acoustic parameter, evaluation noise compensation is applied that includes a truncation of the RIR at the point where the signal decays into the constant noise floor. [7, 8]. This technique is able to remove the consequences of the impulsive noise for low frequencies (in this example for < 400 Hz), due to sufficient time and level distance from the decaying impulse response. This can be further interpreted by looking along the horizontal (constant frequency) impulse response parts (red) decaying into the noise part (blue) without signal and noise overlap. The usage of a robust noise compensation technique for the room acoustic parameter calculation that includes a truncation of the impulse response limits the evaluation errors on the directly affected frequencies, where signal and disruption overlap. For no or other noise compensation techniques, the lower frequencies will also be affected.

Figure 4 shows exemplarily two third octave bands of the energy room impulse response. For the 100 Hz band, the part of the inverse sweep occurs clearly separated from the signal part (Figure 4 top) and is eliminated by the noise compensation method automatically.

For higher frequencies, however, both components overlap and cannot be separated. Around 500 Hz, the inverse

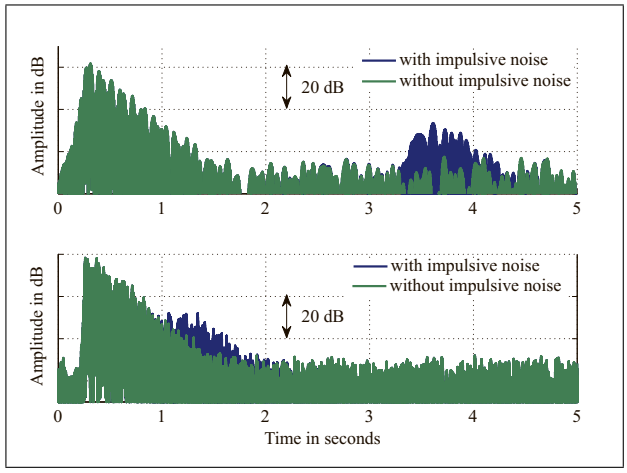


Figure 4. The 100 Hz third octave band (top) and the 500 Hz third octave band (bottom) of the impulse response. The parts of the inverse sweeps appear at different positions in the impulse response and therefore have different impact on the evaluated reverberation time and other room acoustic parameters.

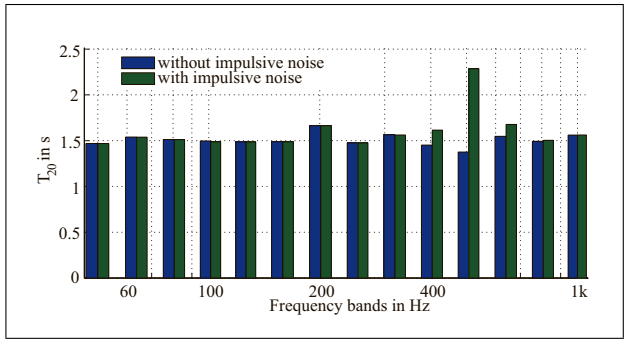


Figure 5. Evaluated reverberation time T_{20} from the simulated impulse response without (green) and with (blue) impulsive noise. This comparison helps to show the effects and is not available in real measurements.

sweep seems to extend the decay of the room (Figure 4 bottom) which results in an overestimated reverberation time (Figure 5). The characteristic of the error has various influence factors: The occurrence of the impulse during the measurement determines the occurrence of the inverse sweep in the RIR and therefore the frequency at which both components overlap. The amplitude of the inverse sweep and the related size of the error are proportional to the amplitude of the impulsive noise. Since the envelope of the inverse sweep is not constant (see Figure 2), an overlap at high frequencies results in larger errors.

3. Detection of impulsive noise

The automatic and reliable detection of the occurrence of an impulsive noise event during the measurement is not trivial. The visibility of the distortion in the final impulse response depends on the level of the impulsive noise, compared to the level of the excitation signal, and on the time when the noise occurs.

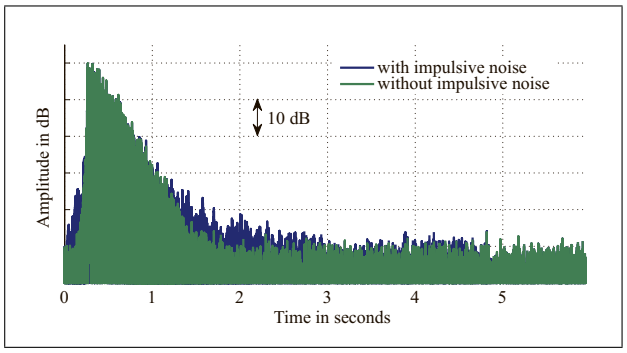


Figure 6. Energy room impulse response with and without an impulsive noise event during the measurement.

In Figure 6, the broadband impulse response of the simulated example is shown, which is evaluated by using Eq.(3). The distortion is visible only in direct comparison to the version without impulsive noise. An automatic detection is not possible in this representation, although the effect on room acoustic parameters is obvious (c.f. Figure 5) for the simulation approach where the noiseless version is known. For real measurements the effect would be similar but it is not possible to identify it as error.

A detection of the impulsive noise directly using the sound pressure level of the recorded microphone signal (before deconvolution) is also very difficult. Despite the constant envelope of the excitation signal, the frequency-dependent transfer functions, which are mainly caused by room (and loudspeaker), lead to strong fluctuations in the envelope of the recorded signal. These temporal fluctuations make it almost impossible to detect impulsive noise reliably. Figure 7 (top) shows the small differences between the time signals caused by the impulsive noise. The impulsive noise is also plotted in yellow for illustration purposes. In the spectrogram of the recorded signal (Figure 7 bottom), the impulsive noise can more easily be visually detected. In this representation, image processing algorithms applied to the spectrogram might be able to detect the impulsive noise as a vertical edge. However, the required signal processing is different from the acoustic and it is difficult to acoustically justify and interpret the thresholds, parameters, and results. The detection method proposed in the following chapter, on the contrary, is based only on ordinary acoustical signal processing and provides physically easily interpretable results (i. e. the estimated background noise).

3.1. Proposed detection algorithm

The dominance of the excitation signal in the recorded microphone signal impedes the detection of impulsive sounds in the recorded signal. Since the excitation signal and at least an estimation of the measured system are known, it is however possible to subtract the signal part from the recorded sequence to obtain an estimation of the background noise.

The best available estimation of the true impulse response $h(t)$ is $h_e(t)$, the early part of the measured impulse response $h_m(t)$ where the signal protrudes above the noise floor. The estimated impulse response $h_e(t)$ can be obtained by applying a time window $w(t)$ to the measured impulse response

$$h_e(t) = h_m(t) \cdot w(t). \tag{4}$$

Here and in the following paper the index "m" refers to a measured signal (including noise components) and "e" refers to estimated signals or systems. The optimal window $w(t)$ fades in at the delay of the system when the impulse response first raises above the noise level, and fades out at the intersection time where the decay of the system intersects with the background noise (see Figure 8). Lundeby et al. [7] developed an iterative algorithm to detect the intersection time automatically. The algorithm has proven to give reliable results even for non-stationary noise and for this reason it is used in this study.

The approach starts with the recorded signal at the microphone position which is the response of the room to the

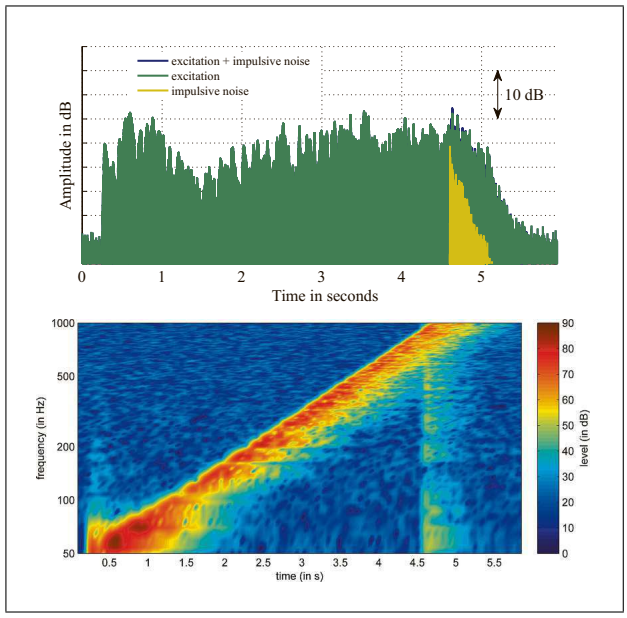


Figure 7. Time signal (top) and spectrogram (bottom) of the recorded signal in the room with an impulsive noise event during the measurement at t = 4.5 s.

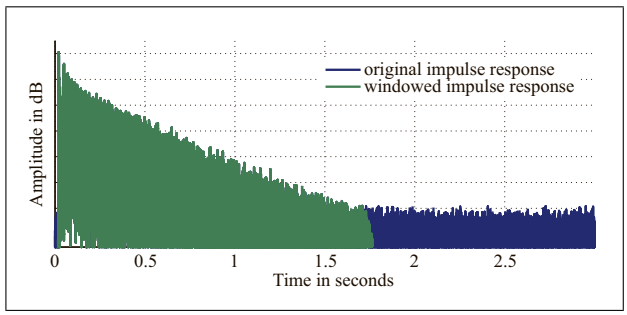


Figure 8. Measured room impulse response before and after windowing (c.f. Equation 4).

excitation signal. The estimated excitation signal recorded at the microphone position, $r_e(t)$ is

$$r_e(t) = h_e(t) * s(t). \tag{5}$$

Since the actual recorded signal $r_m(t)$ is the summation of the room response to the excitation signal and background noise (Equation (2)), it is possible to estimate the background noise $n_e(t)$ by subtraction,

$$n_e(t) = r_m(t) - r_e(t). \tag{6}$$

To simplify the calculation, the noise can be estimated by muting the signal part of the measured impulse response and convolving with the excitation signal,

$$n_e(t) = [h_m(t) \cdot (1 - w(t))] * s(t) \tag{7}$$

The effect of this subtraction technique can be illustrated as follows: The group delay of the sweep increases monotonically from zero, for the start frequency f_1, to the length of the sweep, for the stop frequency f_2. A convolution with the sweep applies a frequency dependent time shift according to this group delay. In this case, the muting time window of Equation (7) is shifted in time depending on the frequency (see Figure 9). This way the excitation signal including its decay is removed from the recorded signal.

The success of this procedure is limited to errors made with the estimation of the system response $h_e(t)$: The true impulse response $h(t)$ continues after the truncation point. This results in remaining signal parts in the estimated background noise. The second error is the noise included in the nominally clean response, despite windowing. This part of the noise cannot be separated from the measured impulse response and will be missing in the estimated background noise. Due to these limitations, a subtraction of the estimated noise from the recorded signal does not provide an advantage. (The subtraction will result in the measured impulse response with a fade-out at the intersection time.) For this reason, perfect noise compensation cannot be achieved with this technique.

Nevertheless, this background noise estimation technique is suitable to detect impulsive noise. It is possible to listen to the background noise estimation and to use a human decision when an impulsive event is present. This procedure is appropriate for single measurements, or for the identification of the noise's source. For a greater number of measurements, an automatic assessment is needed.

A definite decision, whether impulsive noise is present or not, is difficult. The transition is smooth from stationary noise with a lot of impulses with similar amplitude to one impulsive event clearly standing out. The essential question is up to which level one impulsive event has to protrude over the others to have a significant effect for further usage.

Figure 10 shows the estimated background noise for the example RIR. In the estimated noise $n_e(t)$, the impulsive sounds protrude clearly above the stationary background noise and can be easily detected. One simple measure to characterize the impulsive noise in the measurement is

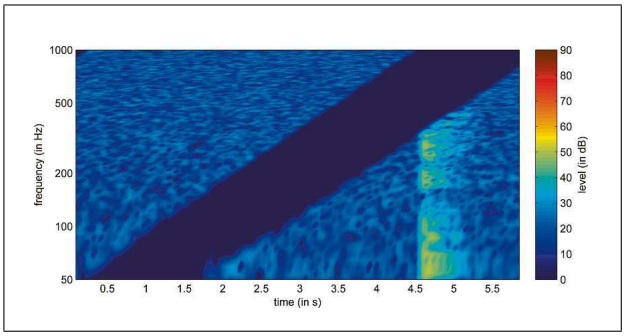


Figure 9. Spectrogram of the estimated background noise. The muting time window of Equation (7) is shifted in time according the frequency dependent group delay of the sweep.

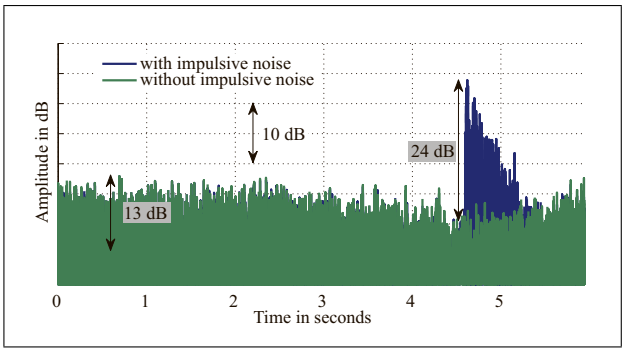


Figure 10. Estimated background noise with (blue) and without (green) impulsive noise according Eq. (7). The Max-RMS ratio is 13 dB without and 24 dB with the impulsive distortion.

$L_{\mathrm{max,rms}}$, the logarithmic ratio of the maximum amplitude of the background noise and the root mean square,

$$L_{\mathrm{max,rms}} = 20 \cdot \log_{10} \frac{\max |n_e(t)|}{\sqrt{\frac{1}{T} \int_0^T |n_e(t)|^2 \, \mathrm{d}t}}. \tag{8}$$

For ideal Gaussian distributed stationary noise free of impulses $L_{\mathrm{max,rms}} = L_{\mathrm{stat}} \approx 12...14$ dB, depending on the number of measured samples. Additional impulsive components in the estimated background noise will cause a greater maximum value, while the root mean square only slightly increases. When the maximum of the pressure is twice the theoretical value (+6 dB), the ratio $L_{\mathrm{max,rms}}$ exceeds around 20 dB and it can be assumed that the disruption has a significant effect on the measurement. For calculated values of $L_{\mathrm{max,rms}}$ around or slightly above L_{stat} , the background noise shows stationary behavior.

Figure 10 shows both estimated background noise signals (with and without impulsive component) calculated using Equation (7). The calculated $L_{\mathrm{max,rms}}$ values are also marked in the figure. With impulsive component, the ratio $L_{\mathrm{max,rms}} = 24$ dB is significantly higher than the theoretical value L_{stat} for stationary noise. Without impulsive component, the ratio $L_{\mathrm{max,rms}} = 13$ dB is in the range of stationary noise.

Comparing the calculated $L_{\mathrm{max,rms}}$ to the theoretical L_{stat} for stationary noise is a suitable indicator for the impulsive noise components within the background noise.

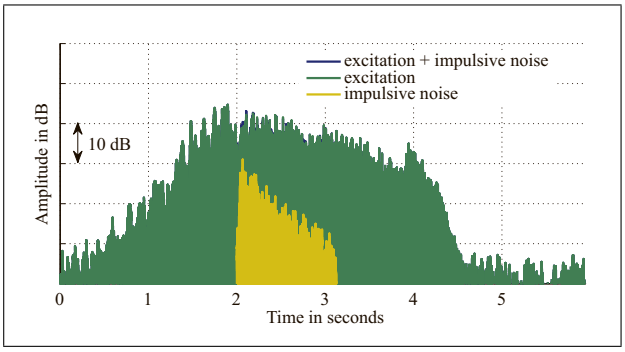


Figure 11. Recorded signal at the microphone position with (blue) and without (green) impulsive noise. The difference of both signals is hardly visible. The impulsive noise is plotted separately for illustration purpose.

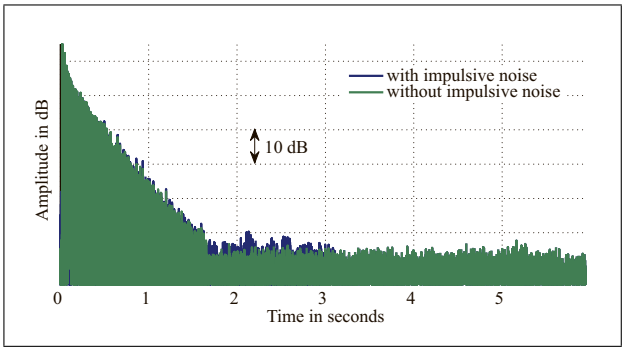


Figure 12. Energy room impulse response of the assembly hall with (blue) and without (green) impulsive noise. The difference can be observed hardly in the middle where the inverse sweep slightly protrudes over the background noise.

In the next chapter, two examples of real measured rooms are shown to demonstrate the procedure and the results under realistic conditions.

4. Experimental validation

The excitation signal and the impulsive noise are recorded separately using the same equipment and same room. The noise is inserted into the measurement subsequently to allow a detailed comparison of all processing steps, comparing the signals with and without impulsive noise components. The complete measurement and room acoustic evaluation is compliant with the ISO 3382 standard [9] and was performed with the ITA-Toolbox [5].

4.1. General assembly hall

The first example is the general assembly hall of RWTH Aachen University. It has a rectangular shape, 600 seats, and a volume of approximately 5500 m^3. It is primarily used for lectures and classical concerts. The dodecahedron loudspeaker was positioned at the stage, and the microphones were located in the audience area. The impulsive noise was produced by a coughing person at a different part of the audience area.

Figure 11 shows a comparison of the recorded signal at the microphone position with (blue) and without (green) impulsive noise. The difference is hardly visible in the envelope. To clarify the position and the amplitude of the disruption, the impulsive noise is plotted separately.

For this scenario, the influence of the impulsive disruptor can be identified clearly at the end of the room impulse response, in comparison to the clean version that only includes stationary noise (see Figure 12). A part of the inverse sweep clearly protrudes above the noise floor.

Figure 13 shows the spectrogram of the impulse response. The low frequency part of the inverse sweep (50 - 400 Hz) overlaps with the impulse response from $t = 0$ s to $t \approx 2$ s (the time of the occurrence of the impulse in the measurement). This part causes large errors in the room acoustic analysis as seen in Figure 14, although this part of the disruption can hardy be detected in the spectrogram.

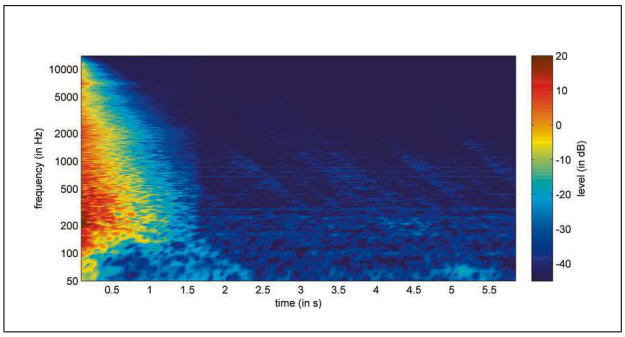


Figure 13. Spectrogram of the disturbed impulse response of the assembly hall.

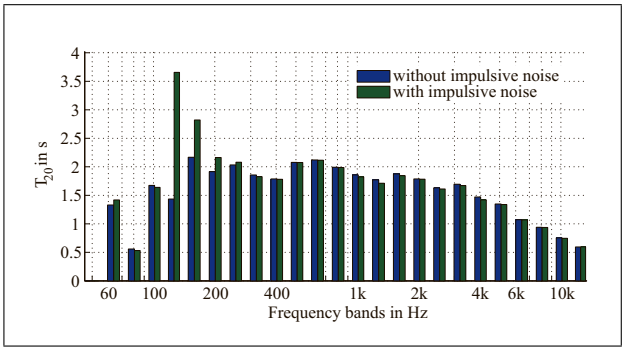


Figure 14. Evaluated reverberation time for the assembly hall measurement. The error occurs only below 400 Hz where signal and noise overlap. This comparison helps to show the effects and is not available in real measurements.

The second part of the inverse sweep (above 400 Hz) appears before $t = 0$ and is usually cut away by the deconvolution process.

Figure 15 shows the estimated background noise for the measurement with and without the impulsive noise component. Now the impulse is clearly visible and the $L_{\mathrm{max,rms}}$ value of about 26 dB indicates a significant disruption. For the case without impulsive noise, the Max-RMS ratio is only 12 dB, which is in the range for stationary noise.

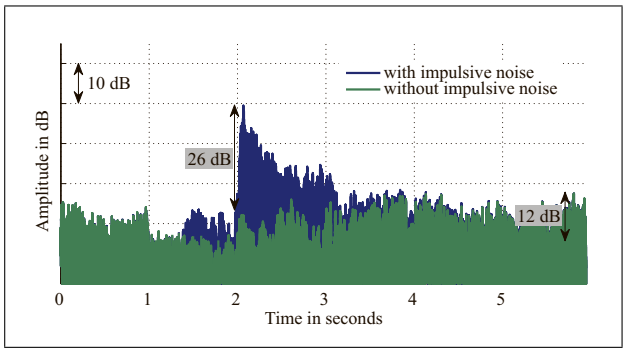


Figure 15. Estimated background noise of measurement with (blue) and without (green) impulsive noise according Equation (7). The Max-RMS ratio increases from 12 dB to 26 dB with the impulsive noise component.

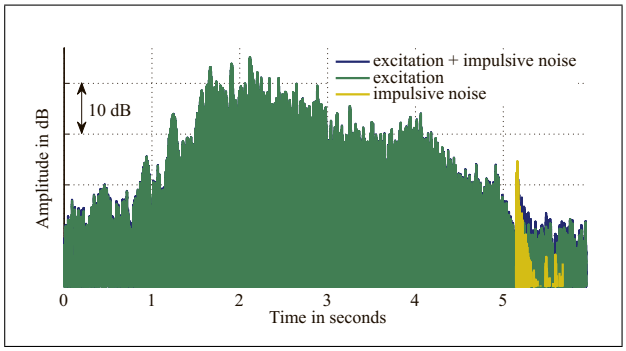


Figure 16. Logarithmic level of the signal recorded at the microphone position. The impulsive noise occurs in the stop margin after the excitation signal at around 5.6 s.

4.2. Ordinary room

The second example is a measurement of an ordinary room. The dimensions of the room are $7 \times 4 \times 2.8\,m^3$. Source and receiver were positioned in different parts of the room. The impulsive noise was produced by dropping a pen from a height of 1.2 m in the middle of loudspeaker and microphone. In this example, the impulsive noise occurs at the end in the stop margin (see Figure 16). The stop margin is the silence part of the excitation signal after the sweep, where the recording is still continued. This part ensures that the last excited frequency components can decay into quiet before the recording period stops.

In this section, impulsive noise often occurs, because persons present in the room may assume that the measurement is already finished and they might cause footstep noise, for example. For the case that the impulsive noise occurs during the stop margin, the inverse sweep in the RIR will never overlap with the direct sound of the impulse response (see Figure 17). Nevertheless, the overlap of the decaying part of the room impulse response with the inverse sweep can significantly affect the room acoustic parameter evaluation. Figure 18 shows that errors of the reverberation time T_{30} above 2 kHz is rising up to more than 100%.

In the estimated background noise, shown in Figure 19, the impulsive noise can be easily identified. The calculated Max-RMS ratio of $L_{\mathrm{max,rms}} = 23$ dB clearly identifies an impulsive component. In comparison, the noiseless version show a value of $L_{\mathrm{max,rms}} = 13$ dB.

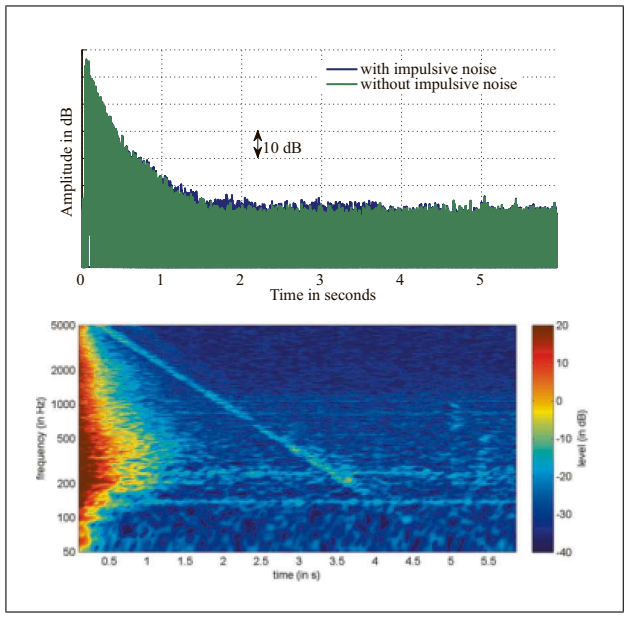


Figure 17. Time signal (top) and spectrogram (bottom) of the disrupted energy room impulse response. In influence of the impulsive noise in the time signal is very small. In the spectrogram the inverse sweep can be seen as a diagonal line from 5 kHz at 0.5 s to 100 Hz at 5 s.

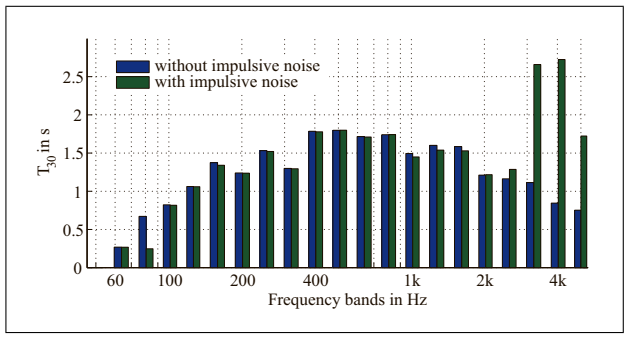


Figure 18. Evaluated reverberation time for the ordinary room without (blue) and with (green) impulsive noise. This comparison helps to show the effects and is not available in real measurements.

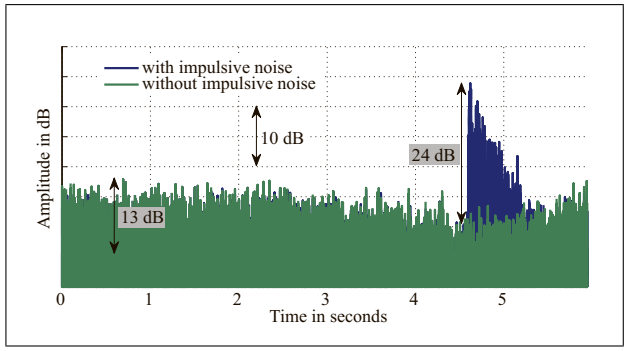


Figure 19. Estimated background noise for the ordinary room according Equation (7). The $L_{\mathrm{max,rms}}$ ratio increases from 13 dB without impulsive noise to 23 dB.

5. Conclusion

This study proposes a method to study impulsive noise in measurements. The motivation of this work is to overcome a disadvantage of sweep measurements, its sensitivity to impulsive noise. Nevertheless, the detection algorithms can be applied to any other excitation signal.

The algorithm estimates and removes the excitation signal component from the recorded signal and supplies the estimated background noise. Based on the estimation, simple quantitative impulsive noise detection is possible. The ratio of the maximum level of the background noise and the mean level is compared to the theoretic value for stationary noise. This technique allows a robust detection of impulsive noise, even if the disruption is not detectable in the room impulse response or the recorded signal and it still has an influence on the room acoustic parameter evaluation. The algorithm is fully automated and does not need any manual adjustment. This allows an automatic analysis directly after the measurement and a repetition of the measurement, if necessary. Furthermore, it is possible to listen to the estimated background noise to allow an individual analysis.

Acknowledgement

This research was funded by the Deutsche Forschungsgemeinschaft (German Research Foundation) DFG as part of the SEACEN research unit (http:// www. seacen. tuberlin.de). The authors would like to thank Pascal Dietrich for many fruitful discussions and the developers of the ITA-Toolbox.

References

[1] G. Stan, J. Embrechts, D. Archambeau: Farina: Comparison of Different Impulse Response Measurement Techniques. J. Audio Eng. Soc, **50** (4) (2002) 249–262.

[2] S. Müller, P. Massarani: Transfer-Function Measurement with Sweeps. J. Audio Eng. Soc **49** (6) (2001) 443–471.

[3] S. Müller: Measuring transfer-functions and impulse responses. Handbook of signal processing in acoustics. Springer New York (2009). 65–85.

[4] A. Farina: Advancements in impulse response measurements by sine sweeps. AES 122nd Convention, Vienna, Austria, 122 **42** (2007).

[5] Institute of Technical Acoustics, RWTH Aachen University: ITA-Toolbox: A MATLAB Toolbox for the needs of acousticians. http://www.ita-toolbox.org/, 2014.

[6] A. Novak, L. Simon, F. Kadlec, P.Lotton: Nonlinear System Identification Using Exponential Swept-Sine Signal. IEEE Transactions on Instrumentation and Measurement **59**(8) (2010) 2220–2229.

[7] A. Lundeby, T. E. Vigran, H. Bietz, M. Vorländer: Uncertainties of measurements in room acoustics. Acta Acustica united with Acustica **81** (1995) 344–355.

[8] M. Guski, M. Vorländer: Comparison of noise compensation methods for room acoustic impulse response evaluations. Acta Acustica united with Acustica **100** (2) (2014) 320–327.

[9] ISO 3382-1: Acoustics – Measurement of room acoustic parameters – Part 1: Performance spaces. International Organization for Standardization (2009).